

PROBING ANOMALOUS TRIPLE GAUGE BOSON  
COUPLINGS IN  $\gamma p \rightarrow ZbX$  PROCESS

I. TURK ÇAKIR

Physics Department, CERN, 1211 Geneva 23, Switzerland  
tcakir@mail.cern.ch*(Received October 13, 2008; revised version received November 6, 2008)*

The prospects of probing anomalous  $Z\gamma\gamma$  and  $ZZ\gamma$  couplings by means of the subprocess  $\gamma q \rightarrow Zb(\bar{b})$  in  $\gamma p$  collisions have been analyzed. The limits on the form factors  $h_3^Z, h_3^\gamma$  and  $h_4^Z, h_4^\gamma$  are obtained for three energy options of the  $\gamma p$  collisions. It is shown that the sensitivity can be reached  $\mathcal{O}(10^{-4})$  if  $b$ -tagging is used.

PACS numbers: 12.60.-i, 12.60.Cn

**1. Introduction**

In the Standard Model (SM) of electroweak and strong interactions, the gauge-bosons interact not only with the matter particles but also with each other. The triple gauge-boson couplings are fundamental prediction of the SM, resulting from the non-Abelian nature of the theory. Experimental high energy physicists have searched for signals of possible deviations of these couplings from the SM structure, either in their form or strength [1]. The precision measurement of the vector boson vertices is crucial and it can reveal the new physics beyond the SM.

Anomalous vertices are an important ingredient in some extended models that allow for composite vector bosons or gauge vector bosons strongly interacting with each other. These interactions manifest themselves as couplings between three (or more) gauge bosons, such as  $ZZ\gamma$ ,  $Z\gamma\gamma$ ,  $WW\gamma$  couplings, referred as triple gauge-couplings (TGC). A considerable effort can be made to increase statistics and improve the sensitivity of the observable to the anomalous couplings at the energies of the proposed high energy colliders. An essential step in this direction can be provided by future  $\gamma p$  collisions.

Anomalous neutral triple gauge couplings (NTGC), which are not present at tree level in the SM, may induce CP-violating effects in some processes  $\gamma e \rightarrow Ze$  [2],  $e^+e^- \rightarrow \gamma Z$  [3],  $e^+e^- \rightarrow ZZ$  [4] and  $pp \rightarrow Z\gamma$  [5]. Experimental limits on these couplings have been provided by the Tevatron

experiments [6]  $|h_3^Z| \leq 0.36$ ,  $|h_4^Z| \leq 0.05$ ,  $|h_3^\gamma| \leq 0.37$ ,  $|h_4^\gamma| \leq 0.05$ , and by Large Electron–Positron (LEP) experiments [7]  $-0.20 \leq |h_3^Z| \leq 0.07$ ,  $-0.05 \leq |h_4^Z| \leq 0.12$ ,  $-0.049 \leq |h_3^\gamma| \leq 0.008$ ,  $-0.002 \leq |h_4^\gamma| \leq 0.034$ . In addition, there are some predictions of triple-gauge boson couplings at the Large Hadron Collider [LHC] [8]. The neutral triple gauge-boson couplings can be measured very accurately at LHC at the level of  $10^{-4}$ – $10^{-7}$ .

In this work, the CP-conserving structure of the  $ZZ\gamma$  and  $Z\gamma\gamma$  vertex is examined through the differential cross-section for the subprocess  $\gamma q \rightarrow Zb(\bar{b})$  (Fig. 1) at a future  $ep$  based  $\gamma p$  collider (see Ref. [9] and references therein) for three energy options  $\sqrt{s_{ep}} = 2.65$  TeV, 3.74 TeV and 6.48 TeV with an integrated luminosity  $L_{ep} = 100$  pb $^{-1}$ . The relevant NTGC vertices are implemented into the program CalcHEP [10]. The total cross-section and angular distribution are obtained for different anomalous couplings. It is shown that the sensitivity to anomalous couplings can be improved if the  $b$ -tagging techniques is used for the final state jet.

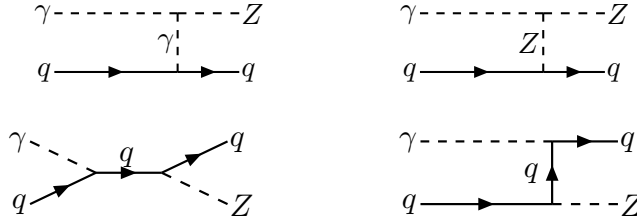


Fig. 1. Feynman diagrams for the  $ZVV$  vertices, where  $V = \gamma, Z$  and  $q = b$  or  $\bar{b}$ .

## 2. $ZVV$ vertices

The most general Lorentz and gauge invariant, CP-conserving  $Z(p_1)\gamma(p_2)Z(p_3)$  vertex in momentum space is given by [11]

$$ig_e \Gamma_{Z\gamma Z}^{\alpha\beta\gamma}(p_1, p_2, p_3) = ig_e \frac{p_3^2 - p_1^2}{m_Z^2} \left[ h_3^Z \varepsilon^{\mu\alpha\beta\rho} p_{2\rho} + \frac{h_4^Z}{m_Z^2} p_3^\alpha \varepsilon^{\mu\beta\rho\sigma} p_{3\mu} p_{2\sigma} \right], \quad (1)$$

where  $m_Z$  is the  $Z$ -boson mass, and  $g_e$  is the electromagnetic coupling. The  $Z\gamma\gamma$  vertex function can be obtained as:

$$ig_e \Gamma_{Z\gamma\gamma}^{\alpha\beta\gamma}(p_1, p_2, p_3) = ig_e \frac{p_3^2}{m_Z^2} \left[ h_3^\gamma \varepsilon^{\mu\alpha\beta\rho} p_{2\rho} + \frac{h_4^\gamma}{m_Z^2} p_3^\alpha \varepsilon^{\mu\beta\rho\sigma} p_{3\mu} p_{2\sigma} \right], \quad (2)$$

where the factor  $p_3^2$  in the  $Z\gamma\gamma$  vertex function comes from the gauge invariance, and it vanishes identically if both photons are on shell (Yang's theorem) due to Bose statistics. These anomalous  $ZZ\gamma$  and  $Z\gamma\gamma$  couplings

must obey Lorentz and gauge invariance. There are eight anomalous coupling parameters  $h_i^Z, h_i^\gamma (i = 1, \dots, 4)$  which are all zero in the SM. CP-even couplings which are proportional to  $h_3^V, h_4^V (V = Z, \gamma)$  are relevant to this study. Due to the partial wave unitarity constraints at the high energies, an energy dependent form factors can be written in the form:

$$h_i^V(\hat{s}) = \frac{h_{i0}^V}{(1 + \hat{s}/\Lambda^2)^3}, \quad i = 1, 3, \quad (3)$$

$$h_i^V(\hat{s}) = \frac{h_{i0}^V}{(1 + \hat{s}/\Lambda^2)^4}, \quad i = 2, 4. \quad (4)$$

The exact form of the form factors depends on the underlying dynamics that generate them and determine the scale  $\Lambda$ . Here  $\Lambda$  is some large energy scale which defines new physics beyond the SM. Usually limits on the parameters are put assuming some large energy scale (commonly infinity). Since the anomalous contribution to the cross-section increase with the center of mass energy, the scale  $\Lambda$  is taken to be the maximal available center of mass energy of the  $\gamma p$  collisions in order to protect the unitarity at high energies.

### 3. Differential cross-section

In general, the differential cross-section for  $\gamma q \rightarrow Zq$  subprocess is given by

$$\frac{d\sigma}{d\cos\theta} = \int_{\tau_{\min}}^{0.83} d\tau \int_{\tau/0.83}^1 \frac{dx}{x} f_{\gamma/e}(\tau/x) f_{q/p}(x, Q^2) \frac{d\hat{\sigma}}{d\cos\theta}, \quad (5)$$

where  $\theta$  is the angle between incoming photon and outgoing  $Z$  boson in the center of mass frame. Here  $\tau_{\min} = (m_Z + m_q)^2/s$ ,  $\tau = \hat{s}/s$ , and  $s$  is the square of the center of mass energy of  $ep$  system. The upper limit of the integral (5) comes from the fact that the energy of converted photons,  $E_\gamma = yE_e$ , is restricted by the Compton backscattering condition  $y_{\max} = 0.83$ . The cross-section can be calculated by integrating over high energy photon spectrum and the quark distribution in the proton. Here, the parton distribution function (pdf) CTEQ6M [12] with the factorization scale  $Q^2 = m_Z^2$  is used. The high energy photon spectrum is given by [13]

$$f_{\gamma/e}(y) = \frac{1}{g(\zeta)} \left[ 1 - y + \frac{1}{1-y} - \frac{4y}{\zeta(1-y)} + \frac{4y^2}{\zeta^2(1-y)^2} \right], \quad (6)$$

where

$$g(\zeta) = \left( 1 - \frac{4}{\zeta} - \frac{8}{\zeta^2} \right) \ln(\zeta + 1) + \frac{1}{2} + \frac{8}{\zeta} - \frac{1}{2(\zeta + 1)^2}, \quad (7)$$

with  $\varsigma = 4.82$ . The total cross-section for the process  $\gamma p \rightarrow Zb(\bar{b})X$  as a function of initial electron beam is shown in Fig. 2. The LHC proton beam energy is taken  $E_p = 7000$  GeV. From this figure it is clear that the cross-section gets a large enhancement due to the anomalous couplings  $h_3^Z, h_3^\gamma$  and  $h_4^Z, h_4^\gamma$ . Especially,  $e^-$  beam energies larger than 100 GeV this enhancement becomes more visible. The cross-section is more sensitive to the anomalous couplings  $h_4^\gamma$  and  $h_4^Z$ . Here the scale  $\Lambda$  is chosen to be the highest centre of mass energy available in  $\gamma p$  collisions in the considered energy range.

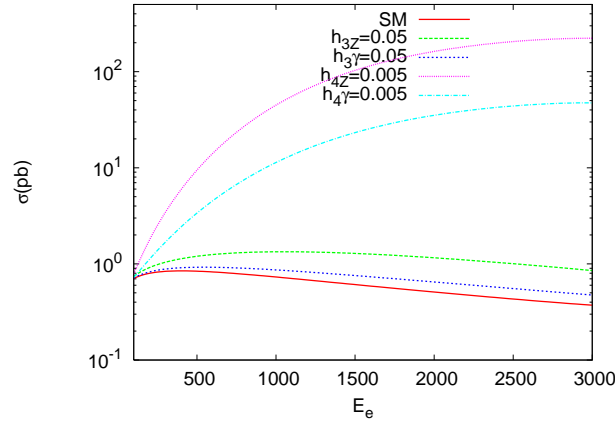


Fig. 2. The total cross-section depending on the energy of the electron beam, for various anomalous couplings. Here proton beam energy is  $E_p = 7000$  GeV.

In the Table I, II and III, the total cross-section for  $\gamma p \rightarrow Zb(\bar{b})X$  is calculated at different electron beam energies  $E_e = 250$  GeV,  $E_e = 500$  GeV and  $E_e = 1500$  GeV. These electron beam energies are planned to be made available at the future linear colliders [14]. From these tables it is clear that the total cross-section is more enhanced at larger anomalous couplings and larger center of mass energies.

TABLE I

The total cross-section values for different couplings at  $E_e = 250$  GeV and  $E_p = 7000$  GeV.

$\sigma(\text{pb})$		$h_4^\gamma$			$h_4^Z$		
		0.01	0.001	0.0001	0.01	0.001	0.0001
$h_3^\gamma$	0.1	3.63	1.19	1.11	10.51	1.27	1.11
	0.01	2.82	0.97	0.95	9.56	1.03	0.95
$h_3^Z$	0.1	4.39	1.81	1.70	13.59	2.12	1.73
	0.01	2.84	0.98	0.95	9.82	1.07	0.96

TABLE II

 The total cross-section values for different couplings  
 at  $E_e = 500$  GeV and  $E_p = 7000$  GeV.

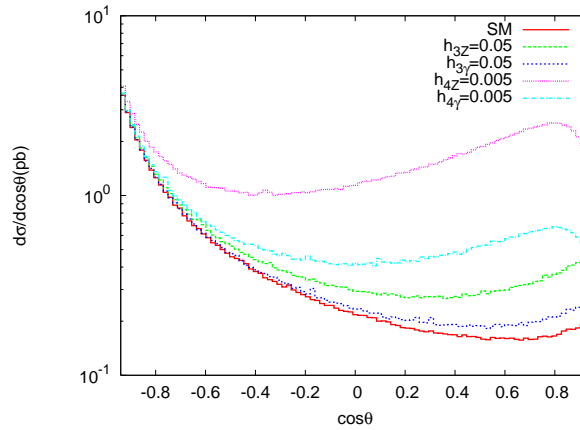
$\sigma(\text{pb})$		$h_4^\gamma$			$h_4^Z$		
		0.01	0.001	0.0001	0.01	0.001	0.0001
$h_3^\gamma$	0.1	19.91	1.81	1.36	77.22	2.45	1.37
	0.01	16.48	1.11	0.93	73.01	1.68	0.94
$h_3^Z$	0.1	22.18	3.37	2.84	90.43	5.09	2.97
	0.01	16.6	1.14	0.95	74.27	1.82	0.96

TABLE III

 The total cross-section values for different couplings  
 at  $E_e = 1500$  GeV and  $E_p = 7000$  GeV.

$\sigma(\text{pb})$		$h_4^\gamma$			$h_4^Z$		
		0.01	0.001	0.0001	0.01	0.001	0.0001
$h_3^\gamma$	0.1	154.43	4.02	1.42	676.88	9.48	1.51
	0.01	141.73	2.13	0.63	660.46	7.33	0.68
$h_3^Z$	0.1	160.09	6.87	3.97	725.14	16.69	4.49
	0.01	141.86	2.19	0.65	665.26	7.82	0.75

It is also important to investigate the angular distribution of the  $b$ -jet in the final state. The behaviour of the differential cross-section is different for the couplings  $h_3^Z, h_3^\gamma$  and  $h_4^Z, h_4^\gamma$ . In Fig. 3, Fig. 4 and Fig. 5, the angular distributions of  $b$ -jet at different center of mass energies are presented. The  $\theta$  is the angle between the incoming and outgoing particles in the center of mass frame. Here, the sensitivity to the couplings  $h_4^\gamma$  and  $h_4^Z$  is more pronounced over the background for large center of mass energies.


 Fig. 3. The differential cross-section depending on  $\cos \theta$  at  $E_e = 250$  GeV and  $E_p = 7000$  GeV.

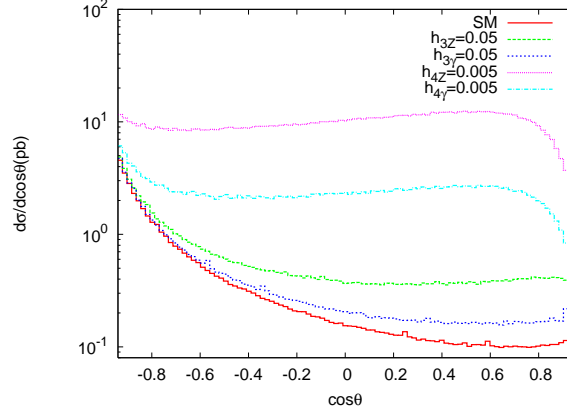


Fig. 4. The differential cross-section depending on  $\cos\theta$ , where  $\theta$  is the angle between incoming and outgoing quarks at  $E_e = 500$  GeV and  $E_p = 7000$  GeV.

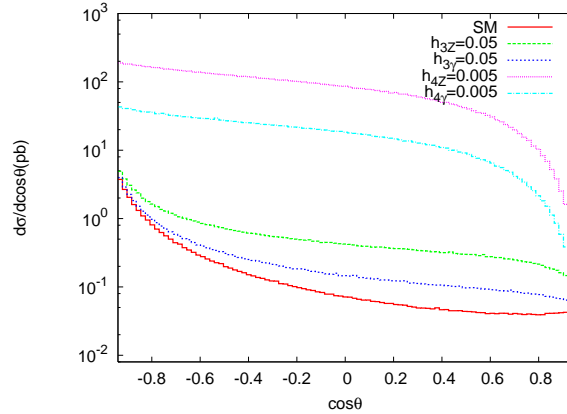


Fig. 5. The differential cross-section depending on  $\cos\theta$  at  $E_e = 1500$  GeV and  $E_p = 7000$  GeV.

#### 4. Limits on the anomalous couplings

In this section, the sensitivity to anomalous couplings is discussed, and the bounds on the  $h_4^V$  and  $h_3^V$  are obtained. The limits at 90% confidence level (C.L.) performing a  $\chi^2$  test for different energy values are calculated. In the calculations a preselection on the angular variable  $\theta$ , as  $|\cos\theta| \leq 0.95$  has been used to regularize the cross-section at small angle. The  $\chi^2$  function contains both the final  $b$ -jet and light-jet mis-tagging contributions. Here,  $b$ -jet tagging efficiency is taken as 60%, with the rejection factors 10 for  $c(\bar{c})$  and 100 for light jets. The  $\chi^2$  function is given by

$$\chi^2 = \sum_i^N \left( \frac{\sigma_{\text{SM}}^i - \sigma_{\text{SM+A}}^i}{\Delta\sigma_{\text{SM}}^i} \right)^2, \quad (8)$$

where  $\sigma_{\text{SM}}^i$  is the cross-section for the SM background in the  $i$ -th bin. It includes both  $b$ -jet and light-jet contributions with the corresponding efficiency factors.  $\Delta\sigma_{\text{SM}}^i$  is the estimated error on the background cross-section. It is given by  $\Delta\sigma_{\text{SM}} = \sigma_{\text{SM}} \sqrt{\delta_{\text{stat.}}^2 + \delta_{\text{sys.}}^2}$  with  $\delta_{\text{stat.}} = 1/\sqrt{N_{\text{SM}}}$  and  $\delta_{\text{sys.}} = 0.05$ . The number of the events for the corresponding background is calculated as  $N_{\text{SM}} = \sigma \times \varepsilon \times L_{\text{int}}$ , where  $L_{\text{int}}$  is the integrated luminosity per year and  $\varepsilon$  is the overall efficiency factor.

In Table IV, we obtain a sensitivity to anomalous couplings  $h_3^Z = 5.63 \times 10^{-3}$ ,  $h_3^\gamma = 9.19 \times 10^{-2}$  and  $h_4^Z = 4.12 \times 10^{-5}$  and  $h_4^\gamma = 6.38 \times 10^{-5}$  at  $\sqrt{s} = 6.48$  TeV and  $L_{\text{int}} = 100\text{fb}^{-1}$ . In Table IV, the results are given for only  $b$ -jet in the final state, if we make an analysis taking into account the mis-tagging of light jets as the  $b$ -jets, then the results will slightly changes as in Table V. Here the reachable bounds on the couplings  $h_3^Z = 6.41 \times 10^{-3}$ ,  $h_3^\gamma = 10.1 \times 10^{-3}$  and  $h_4^Z = 4.47 \times 10^{-5}$  and  $h_4^\gamma = 7.00 \times 10^{-5}$ . The contribution of the  $\gamma p \rightarrow Zb(\bar{b})X$  process to background cross-section is 0.94 (0.92) [0.59] pb at  $\sqrt{s} = 2.65$  (3.74) [6.48] TeV and one another contribution from  $\gamma p \rightarrow Zc(\bar{c})X$  process is 5.19 (4.88) [3.05] pb at  $\sqrt{s} = 2.65$  (3.74) [6.48] TeV, respectively. Furthermore,  $\gamma p \rightarrow ZjX$  (where  $j$  is a light jet including  $u, d, s$  quarks and their anti-quarks), contribution 15.38 (13.01) [7.57] pb at  $\sqrt{s} = 2.65$  (3.74)[6.48]. The search limits on anomalous couplings benefit from the  $b$ -tagging. Contributions from the all jets slightly changes the bounds achievable at  $\gamma p$  collisions.

TABLE IV

Sensitivity of the  $\gamma p$  collider to  $Z\gamma\gamma$  and  $ZZ\gamma$  couplings at 90% C.L, at  $\sqrt{s} = 2.65, 3.74, 6.48$  TeV and  $L_{\text{int}} = 100 \text{ fb}^{-1}$ . Only one of the couplings is assumed to deviate from the SM at a time. The values corresponds to the calculation for  $b$ -jet in the final state.

$\sqrt{s}(\text{TeV})$	$h_3^Z$	$h_3^\gamma$	$h_4^Z$	$h_4^\gamma$
2.65	$1.56 \times 10^{-2}$	$2.57 \times 10^{-2}$	$4.43 \times 10^{-4}$	$8.88 \times 10^{-4}$
3.74	$9.08 \times 10^{-3}$	$1.50 \times 10^{-2}$	$1.44 \times 10^{-4}$	$2.25 \times 10^{-4}$
6.48	$5.63 \times 10^{-3}$	$9.19 \times 10^{-2}$	$4.12 \times 10^{-5}$	$6.38 \times 10^{-5}$

TABLE V

Sensitivity of the  $\gamma p$  collisions to  $Z\gamma\gamma$  and  $ZZ\gamma$  couplings at 90% C.L., for  $\sqrt{s} = 2.65, 3.74, 6.48$  TeV and  $L_{\text{int}} = 100 \text{ fb}^{-1}$ . Only one of the couplings is assumed to deviate from the SM at a time there, the signal and background are calculated taking into account contributions from tagged  $b$ -jet and mis-tagged light jets.

$\sqrt{s}(\text{TeV})$	$h_3^Z$	$h_3^\gamma$	$h_4^Z$	$h_4^\gamma$
2.65	$4.57 \times 10^{-2}$	$2.57 \times 10^{-2}$	$4.40 \times 10^{-4}$	$7.01 \times 10^{-4}$
3.74	$9.66 \times 10^{-3}$	$1.51 \times 10^{-2}$	$1.45 \times 10^{-4}$	$2.25 \times 10^{-4}$
6.48	$6.41 \times 10^{-3}$	$10.1 \times 10^{-3}$	$4.47 \times 10^{-5}$	$7.00 \times 10^{-5}$

## 5. Conclusions

The precision measurement of the vector boson couplings is very important for the future experiments, and it can point the new physics beyond the SM. The neutral triple gauge couplings can be tested at different lepton and hadron colliders. As a complementary environment,  $\gamma p$  collisions can give valuable physics contributions to the same searches. This work shows that higher center of mass energy will be useful for investigation of anomalous gauge couplings provided these are not too small to be probed in the foreseen  $\gamma p$  colliders.

I would like to thank G. Unel, O. Cakir, A. Pukhov and A. Belyaev for their contributions and valuable discussions. I would also like to thank CERN Physics Department for giving me the opportunity to study there.

## REFERENCES

- [1] C. Amsler *et al.*, *Phys. Lett.* **B667**, 411 (2008).
- [2] T.G. Rizzo, *Phys. Rev.* **D54**, 3057 (1996); S. Atag, I. Sahin, *Phys. Rev.* **D68**, 093014 (2003).
- [3] D. Choudhury, S.D. Rindani, *Phys. Lett.* **B335**, 198 (1994); S. Atag, I. Sahin, *Phys. Rev.* **D70**, 053014 (2004); B. Ananthanarayan, S.D. Rindani, *J. High Energy Phys.* **10**, 077 (2005); A. Gutierrez-Rodriguez, M.A. Hernandez-Ruiz, M.A.Perez, 0808.0945 [hep-ph]; M.A Perez, F. Ramirez-Zavaleta, *Phys. Lett.* **B609**, 68 (2005).
- [4] D. Change, W.Y. Keung, P.B. Pal, *Phys. Rev.* **D51**, 1326 (1995); J. Biebel, *Phys. Lett.* **B448**, 125 (1999).
- [5] S. Dawson, X.-G. He, G. Valencia, *Phys. Lett.* **B390**, 431 (1997); U. Baur, E.L. Berger, *Phys. Rev.* **D47**, 4889 (1993).
- [6] [DØ Collaboration], B. Abbott *et al.*, *Phys. Rev.* **D57**, R3817 (1998).

- [7] S. Villa, *Nucl. Phys.* **B142**, 391 (2005).
- [8] S. Hassani, *Czech. J. Phys.* **54**, A239 (2004).
- [9] S. Sultansoy, *Eur. Phys. J.* **C33**, 1064 (2004).
- [10] A. Pukhov, [hep-ph/0412191](#).
- [11] U. Baur, E.L. Berger, *Phys. Rev.* **D47**, 4889 (1993); K. Hagiwara *et al.*, *Nucl. Phys.* **B282**, 253 (1987); F.M. Renard, *Nucl. Phys.* **B196**, 93 (1982).
- [12] J. Pumplin *et al.*, *J. High Energy Phys.* **0207**, 012 (2002).
- [13] I.F. Ginzburg *et al.*, *Nucl. Instrum. Methods Phys. Res.* **205**, 47 (1983); *Nucl. Instrum. Methods Phys. Res.* **A219**, 5 (1984); V.I. Telnov, *Nucl. Instrum. Methods Phys. Res.* **A294**, 72 (1990); D.I. Borden, D.A. Bauer, D.O. Caldwell, SLAC Report No. SLAC-PUB-5715, Stanford 1992.
- [14] G.A. Loew, Report from the ILC technical review committee, Slac-pub-10024 (2003); A comprehensive information about the future linear colliders can be found at the URL: <http://www.linearcollider.org>; E. Accomando *et al.*, Report of the CLIC Physics Working Group, CERN-2004-005, Geneva 2004; [hep-ph/0412251](#).